Acta Oceanol. Sin., 2018, Vol. 37, No. 4, P. 109–121
DOI: 10.1007/s13131-017-1129-5
http://www.hyxb.org.cn
E-mail: hyxbe@263.net

Regional disparities of phytoplankton in relation to environmental factors in the western Arctic Ocean during summer of 2010

LIN Gengming[1]*, WANG Yanguo[1], CHEN Yanghang[1], YE Youyin[1], WANG Yu[1], YANG Qingliang[1]

[1] Third Institute of Oceanography, State Oceanic Administration, Xiamen 361005, China

Received 28 March 2017; accepted 4 August 2017

Abstract

Global warming has caused Arctic sea ice to rapidly retreat, which is affecting phytoplankton, the primary producers at the base of the food chain, as well as the entire ecosystem. However, few studies with large spatial scales related to the Arctic Basin at high latitude have been conducted. This study aimed to investigate the relationship between changes in phytoplankton community structure and ice conditions. Fifty surface and 41 vertically stratified water samples from the western Arctic Ocean (67.0°–88°26′N, 152°–178°54′W) were collected by the Chinese icebreaker R/V *Xuelong* from July 20 to August 30, 2010 during China's fourth Arctic expedition. Using these samples, the species composition, spatial distribution, and regional disparities of phytoplankton during different stages of ice melt were assessed. A total of 157 phytoplankton taxa (>5 μm) belonging to 69 genera were identified in the study area. The most abundant species were *Navicula pelagica* and *Thalassiosira nordenskioeldii*, accounting for 31.23% and 14.12% of the total phytoplankton abundance, respectively. The average abundance during the departure trip and the return trip were 797.07×10^2 cells/L and 84.94×10^2 cells/L, respectively. The highest abundance was observed at Sta. R09 in the north of Herald Shoal, where *Navicula pelagica* was the dominant species accounting for 59.42% of the abundance. The vertical distribution of phytoplankton abundance displayed regional differences, and the maximum abundances were confined to the lower layers of the euphotic zone near the layers of the halocline, thermocline, and nutricline. The species abundance of phytoplankton decreased from the low-latitude shelf to the high-latitude basin on both the departure and return trips. The phytoplankton community structure in the shallow continental shelf changed markedly during different stages of ice melt, and there was shift in dominant species from centric to pennate diatoms. Results of canonical correspondence analysis (CCA) showed that there were two distinct communities of phytoplankton in the western Arctic Ocean, and water temperature, ice coverage and silicate concentration were the most important environmental factors affecting phytoplankton distribution in the surveyed sea. These findings will help predict the responses of phytoplankton to the rapid melting of Arctic sea ice.

Key words: phytoplankton, regional disparity, species composition, spatial distribution, western Arctic Ocean

Citation: Lin Gengming, Wang Yanguo, Chen Yanghang, Ye Youyin, Wang Yu, Yang Qingliang. 2018. Regional disparities of phytoplankton in relation to environmental factors in the western Arctic Ocean during summer of 2010. Acta Oceanologica Sinica, 37(4): 109–121, doi: 10.1007/s13131-017-1129-5

1 Introduction

High-latitude marine ecosystems are particularly sensitive to climate change because small temperature differences have large effects on the extent and thickness of sea ice (Holland et al., 2006a). Over recent years, the Arctic Ocean has experienced a reduction in sea ice cover (10% loss per decade for 1979–2006; Comiso et al., 2008; Polyakov et al., 2010) and thickness (over 50% reduction in ice volume; Kwok and Rothrock, 2009). These values reached their lowest in 2007 and 2011 (Perovich, 2011). Models predict that sea ice will continue to shrink in the coming years and that near ice-free conditions could occur by the summer of 2040 (Holland et al., 2006b; Overland and Wang, 2007). In the Arctic, rising air temperature, increasing precipitation, larger river flows, and decreasing snow cover have led to large and rapid changes in the upper ocean (Li et al., 2009). The recent exceptional decline and thinning of Arctic sea ice caused by increasing greenhouse gases emissions have placed the Arctic Ocean at the center of international scientific attention (Wassmann et al., 2011). The rapid environmental changes occurring in the Arctic Ocean are altering ecological patterns. Climate-driven biological impacts included large changes in species diversity, primary productivity, geographic range of species shifting into and out of the Arctic, and community restructuring (Cronin and Cronin, 2015). Satellite observations suggest an increase in primary production and phytoplankton biomass relative to an increase of open-water area and longer ice-free periods correspond to a longer phytoplankton growing season (Arrigo et al., 2008; Pabi et al., 2008). The timing and species composition of the spring bloom of phytoplankton appears to have been delayed by early ice retreat in the Bering Sea (Hunt Jr et al., 2002). The Labrador Sea spring and early summer blooms are composed of contrasting phytoplankton communities, for which taxonomic segregation ap-

Foundation item: The Public Science and Technology Research Funds Projects of Ocean under contract No. 201305027; the National Natural Science Foundation of China under contract No. 41306204.
*Corresponding author, E-mail: lingengming@tio.org.cn

pears to be controlled by the physical and biogeochemical characteristics of the dominant water masses (Fragoso et al., 2016). Phytoplankton biomass increased much earlier in the Beaufort Sea when sea ice decreased early in the year, and annual chlorophyll fluctuations showed biomass peaks up to 2 months later in cold years accompanied by more extensive ice cover (Wang et al., 2005). With record levels of ice retreat observed in the early 21st century (ACIA, 2005; Stroeve et al., 2005), a northward shift of the subarctic/arctic boundary is possible, together with the northward migration of competitive species into the warmer environments (Grebmeier et al., 2006b). This is because global climate changes conditions will favor some organisms more than others; with the smallest phytoplankton cells thriving, but larger cells languishing in the changing Arctic Ocean (Li et al., 2009). In the Chukchi Sea and its adjacent waters, microphytoplankton have been shown to be sensitive to the environmental changes and exhibit a drastic reduction of the chlorophyll content, while the chlorophyll *a* content of nanophytoplankton and picophytoplankton do not change considerably (Le et al., 2014). In the Arctic Melting Zone at 78°–82°N, the drastic reduction of ice cover from (95±4)% in 1994 to (40±36)% in 2008 caused a rapid growth of nanoplankton and microplankton, while the picoplankton abundance decreased by a factor of 10–20 folds (Coupel et al., 2011). In these newly open surface waters near the Alpha-Mendeleev Ridge and Makarov Basin, Chlorophyll *a* concentrations were low, and picophytoplankton dominated these areas (Zhang et al., 2015). In contrast, a reduction in nanophytoplankton but an increase in picophytoplankton was recorded in the Canada Basin from 2004 to 2008 (William et al., 2009). It is understood that there is a large difference in various phytoplankton groups response to rapidly declining ice cover (ice retreat) across the different regions of the Arctic Ocean.

Only very limited and fragmented phytoplankton data are available from the high latitude western Arctic Ocean due to limited access to these ice-covered seas. The most studied areas are the Chukchi Shelf (Kiselev, 1937; Bursa, 1963; Hameedi, 1978; Okolodkov, 1987; Wang et al., 2005), and the shelf break and slope area (Horner, 1984; Booth and Horner, 1997; Grebmeier, 2003; Grebmeier and Harvey, 2005; Hill and Cota, 2005; Hill et al., 2005; Sukhanova et al., 2009; Sergeeva et al., 2010). These studies mainly described the taxonomic composition, abundance, biomass, primary productivity, spatial distribution, and seasonal variability of phytoplankton. Only a few oceanographic projects have involved large-scale latitudinal changes. For example, the Arctic Ocean Section in summer 1994, the Surface Heat Budget of the Arctic 1997, the Shelf-Basin Interactions Program in summer 2002, the Russian–American Long-term Census of the Arctic 2004, and the Pan-Arctic Beringia 2005 took place in the high Arctic latitudes. However, in these studies, the taxonomic composition of phytoplankton was analyzed by size fractionation and high-performance liquid chromatography analysis of pigments; the quantitative characteristics were estimated only from the chlorophyll *a* concentrations (Gosselin et al., 1997; Zapata et al., 2000). Although identification by light microscopy is time-consuming and requires a high level of taxonomic skills, it is still the most reliable method of microalgal identification (Tomas, 1997; Bérard-Therriault et al., 1999).

The Chinese National Arctic Research Expedition (CHINARE) undertook a series of oceanographic campaigns (1999, 2003, 2008, 2010, 2012, and 2014) on the icebreaker R/V *Xuelong*. The first two investigative voyages were only conducted in the Bering Sea, the Chukchi Sea, and the southern Canadian Basin. In 2008, the voyage extended to 86°N. However, Chinese scholars reported the species composition and distribution of net-phytoplankton (Yang et al., 2002; Yang and Lin, 2006; Lin et al., 2009), as well as the primary productivity and size-fractionated chlorophyll *a* concentration of phytoplankton (Liu et al., 2007, 2011), only in the Bering Sea, the Chukchi Sea, and the northern Chukchi Plateaus. International investigators such as Coupel et al. (2011, 2012) and Joo et al. (2012) investigated phytoplankton communities in a larger area, up to 86°N towards high latitude, and they mainly studied the distribution, composition, chlorophyll *a* concentrations of size-fractionated phytoplankton and their contribution to total abundance and bio-volume. The sampling of water stratifications was only conducted at surface and subsurface of chlorophyll *a* at maximum depths. In 2010, the voyage extended to extremely high latitudes (88°26′N) for the first time, with only the species diversity of surface phytoplankton communities reported (Lin et al., 2013). The present study further analyzed the vertical distributions, regional disparities, and species variations of phytoplankton at different stages of ice melting in the area of the western Arctic Ocean. In addition, the spatial heterogeneity of phytoplankton communities was studied in terms of large-scale latitudinal changes, and its relation to the principal abiotic conditions. This study was to evaluate the effects of ice retreat on the phytoplankton assemblages to provide a scientific basis for predicting the effects of global warming on the Arctic ecosystems.

2 Materials and methods

2.1 *Study sites*

The study region encompassed an area between 67.0°–88°26′N and 152°–178°54′W, and was divided into three geographical provinces based on bathymetry: the shallow continental shelf, the continental slope, and the deep ocean. The shallow continental shelf was at a depth of less than 100 m, including Chukchi Shelf and the Alaska's northwest coast. The continental slope was located in the northern and northeastern parts of the Chukchi Sea at a depth of 100–500 m, included the Chukchi Abyssal Plain, the Chukchi Cap and the Northwind Ridge. The deep ocean was at a depth of 500–4 000 m, included the Canadian Abyssal Basin, the Mendeleev Abyssal Plain and Alpha Ridge. The 50 phytoplankton sampling stations included 23 stations in the shallow continental shelf, five stations in the continental slope and 22 stations in the deep ocean. Based on the geographical location, as well as the hydrological and investigation time, six stations representing different latitudes and depths were selected to analyze the regional disparity in the vertical distribution of phytoplankton (Fig. 1).

2.2 *Sampling and analysis*

The study was conducted between July 20, 2010 and August 30, 2010, as part of CHINARE 2010, aboard the Chinese icebreaker R/V *Xuelong*. One liter Phytoplankton samples were collected using 10 L Niskin bottles at 50 stations in three regions. A total of 91 water samples were collected, including 50 surface and 41 vertical stratified samples collected from eight depths (10, 20, 30, 50, 75, 100, 150, and 200 m) depending on the water depth. All samples were immediately fixed with Lugol's solution (final concentration of 2%). After 24 h, buffered formaldehyde was added (final concentration 2%). Determinations and counts of 25 mL subsamples were analyzed under an inverted Zeiss-Z1 microscope (Carl Zeiss MicroImaging, Göttingen, Germany) at 200× or 400× magnification using the Utermöhl method (Utermöhl, 1958). Identification of algal species was based on Round et al.

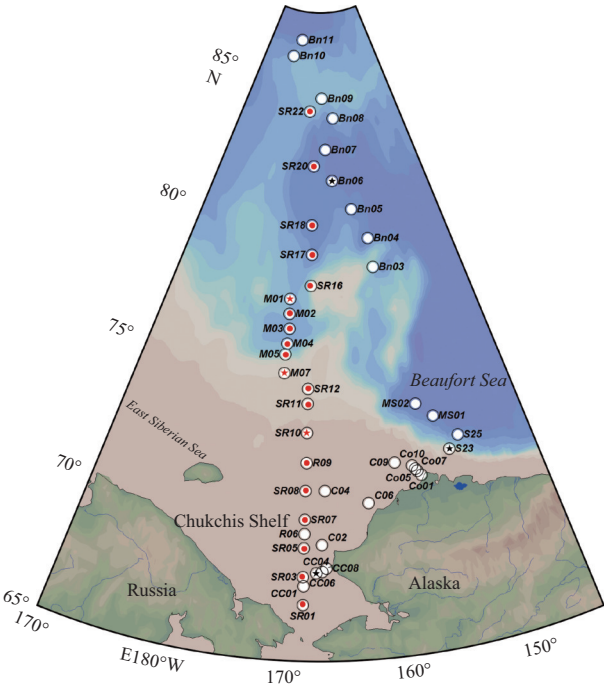

Fig. 1. Locations of sample stations. Hollow circles (○) and solid (◉) indicate 30 departing trip stations (sampled from July 20 to August 6) and 20 return trip stations (sampled from August 22 to 30), respectively. Among them, star (★) indicates six vertically stratified collection stations.

(1990), Tomas (1997), Sun and Liu (2002), and Lee (2008). Temperature and salinity data were collected using a Sea-Bird 911 CTD probe (Seabird Electronics, Inc., Bellevue, WA, USA). Nutrient samples were collected using Niskin water bottles and processed using a Model 300 automated nutrient analyzer (Alpkem, Clackamas, OR, USA; Grasshoff et al., 1999). The ice coverage was visually estimated from the bridge of the R/V *Xuelong*.

The species data were $\log_{10}(x+1)$ transformed before analysis to obtain consecutive distributions. The species richness (d) and species dominance (Y) were calculated using the following formulae:

$$d = (S-1)/\log_2 N,\ \ Y = (n/N)\times f,$$

where n is the number of organisms of the i species, N is the total number of organisms in the sample, f is the occurrence frequency of i species, and S is the species number in the sample.

Relationships between phytoplankton community and environmental variables were analyzed by CANOCO version 4.5. Only those taxa that were observed in more than 10% of the samples and with more than 1% in the total abundance were included in analyses. Both of the species data and the environmental variables were $\log_{10}(x+1)$ transformed before analyses. Detrended correspondence analysis (DCA) for the species data was used to determine the methods that would be applied. As was suitable for unimodal ordination, canonical correspondence analysis (CCA) was chosen since that the maximum gradient length of the four axes was between 3 and 4.

3 Results

Since the investigation lasted more than a month, the environmental conditions (e.g., ice conditions, water temperature, salinity, and nutrients) and phytoplankton distribution changed dramatically between the departing and the return trips. Moreover, the water depth, hydrodynamics, and geographic conditions of different regions (i.e., the shallow continental shelf, the continental slope, and the deep ocean) varied significantly. To facilitate the comparison of spatial heterogeneity of phytoplankton distribution in different regions and better illustrate relationship between the characteristics of phytoplankton distribution and related environmental factors, we separated the results observed during the departing and return trips, and sequentially described the results from the shallow continental shelf, the continental slope, and the deep ocean (Table 1).

3.1 *Physico-chemical parameters*

During the departure trip from July 20 to August 6, 2010, ice conditions worsened from the shallow continental shelf to the continental slope and further into the deep ocean, the coverage and thickness of sea ice gradually decreased. Most of the Chukchi Shelf became an ice-free area. Only seven out of 16 stations were covered with ice. In the eastern Chukchi Sea and in the northwest of Point Barrow, ice coverage exceeded 80%. Stations R08 and R09 near the Herald Shoal were located at the ice edge. All 12 stations in the deep ocean were completely covered with ice.

The water temperature decreased significantly as the voyage proceeded north. The temperature in the shallow continental shelf was relatively high. The temperature in the southern Chukchi Sea was approximately 5°C. The temperature in the continental slope declined nearly to 0°C. The temperature in the deep ocean fell further to below 0°C, ranging from –1.53 to –0.19°C.

The distribution pattern of salinity was consistent with temperature. Salinity in the southern Chukchi Sea was the highest (31.0). Salinity declined significantly along the continental slope. Salinity in the deep ocean was relatively low, ranging from 25.97 to 30.64. It increased from the southern to the northern parts of this region, salinity in the southern Canadian Basin was below 27.0, with minimum salinity (25.96) recorded at Sta. MS02, and salinity in the northern area of the western Arctic Ocean was above 30.0, with maximum salinity (30.64) recorded at Sta. Bn11 in the northern Alpha Ridge.

Nutrients in the shallow continental shelf were abundant; levels were lower in the south than in the north. The nutrient concentrations in the southern Chukchi Sea and along the coast of Alaska were relatively low. The silicate concentration at Sta. R03 was 0.01 μmol/L, and the dissolved inorganic nitrogen (DIN) concentration at Sta. CC08 was 0.11 μmol/L, which were the lowest in this region. The nutrient concentration in the northern Chukchi Sea was relatively high. The silicate concentration at Sta. R08 was 19.00 μmol/L, and the phosphate concentration at Sta. R09 was 0.72 μmol/L, the highest in this region. Nutrient concentrations at two stations in the continental slope were similar. The distribution of nutrient concentration across the entire deep ocean was relatively even, except for the particularly high silicate concentration at Stas Bn10 and Bn11.

During the return trip in August 22–30, 2010, most of the sea ice had melted, with ice-free conditions in the shallow continental shelf and in the continental slope. Although the ten stations in the deep ocean were covered with ice, the ice coverage had reduced, with more than 70% ice coverage at Stas SR18, SR20 and SR22 in the northern Mendeleev Abyssal Plain and less than 50% ice coverage at Stas SR16 and SR17 in the southern Mendeleev Abyssal Plain. Ice coverage at Stas M01, M02, M03, M04 and M05 in Chukchi Abyssal Plain was between 10%–30%.

Table 1. Position, depth, ice condition, nutrient content, hydrology and phytoplankton community structure data for different regions in the western Arctic Ocean during the summer of 2010

	Cruises					
	Departing trip			Return trip		
Date	Jul. 20–25, 2010	Jul. 25–26, 2010	Jul. 26–August 6, 2010	Aug. 22–28, 2010	Aug. 25–29, 2010	Aug. 29–30, 2010
Region	shallow continental shelf	continental slope	deep ocean	continental slope	shallow continental shelf	
Station	R03, CC01, CC04, CC06, CC08, C02, C04, C06, C09, CO10, R06, R08, R09, CO01, CO03, CO07	CO05, S23	S25, MS01, MS02, Bn03, Bn04, Bn05, Bn06, Bn07, Bn08, Bn09, Bn10, Bn11	M01, M02, M03, M04, M05, SR16, SR17, SR18, SR20, SR22	SR11, SR12, M07	SR01, SR03, SR05, SR07, SR08, SR09, SR10
Depth/m	<100 (34–93)	<500 (116–360)	>500 (2 455–3 898)	>500 (657–3 460)	<500 (171–381)	<100 (37–77)
Ice coverage/%	26.25±37.57	60±28	77.5±20	44.5±39.6	3.33±5.77	0
Ice height/m	0–1.0	1.0	1.0–1.6	0.6–1.3	0.0–0.8	0.0
Salinity	30.81±0.94	29.32±0.98	28.81±1.57	27.69±1.43	27.30±0.36	30.56±1.08
Water temperature/°C	3.43±2.80	0.57±1.35	–1.19±0.55	–1.26±0.20	0.38±0.99	5.02±1.79
Phosphate/μmol·L^{-1}	0.46±0.16	0.58±0.07	0.58±0.15	0.64±0.06	0.70±0.04	0.47±0.26
DIN/μmol·L^{-1}	0.40±0.28	0.57±0.15	0.52±0.57	0.29±0.15	0.52±0.12	1.02±1.63
Silicate/μmol·L^{-1}	3.39±5.30	0.83±0.80	2.78±2.43	2.09±1.23	2.61±0.16	4.44±6.18
Abundance/10^2 cells·L^{-1}	1 466.99±3 390.41	51.88±5.48	27.65±18.67	9.70±7.99	12.41±6.29	223.12±275.68
Dominant species[1)]	*Navicula pelagic*, *Thalassiosira nordenskioedii*, *Pseudo-nitzschia seriata*	*Navicula pelagic*, *Chaetoceros concavicornus*	*Thalassionema nitzschioides*, *Eutreptiella gymnastica*, *Alexandrium ostenfeldii*	*Thalassionema nitzschioides*, *Eutreptiella gymnastica*, *Protoperidinium bipes*	*Thalassiosira nordenskioedii*, *Chaetoceros furcellatus*	*Chaetoceros diadema*, *Letocylindrus danicus*, *Navicula pelagic*, *Cylindrotheca closterium*
Proportion of diatom to total abundance/%	96.74	94.58	78.02	80.18	95.18	98.04
Proportion of dinoflagellate to total abundance/%	1.88	3.65	7.08	5.98	3.36	1.46
Species richness (d)	2.07±0.83	1.81±0.9	1.55±0.54	0.95±0.58	0.97±0.26	1.87±0.60

Note: [1)] Values of dominant index are greater than 0.02.

The temperature in the three regions was significantly elevated. The temperature in the shallow continental shelf ranged from 1.76°C to 7.81°C. Stations SR10 in the northern Chukchi Sea and Sta. SR05 in the center of the Chukchi Sea had the lowest and highest temperatures, respectively. The temperature in other stations was approximately 5.0°C. Average temperature in the continental slope was above 0°C. Temperatures increased from northern to southern regions. The lowest and highest temperatures were found at Sta. M07 in the Chukchi Abyssal Plain (–0.72°C) and at Sta. SR11 in the continental slope of the Chukchi Sea (1.21°C), respectively. The average temperature in the deep ocean ranged from –1.55°C to –1.03°C, increasing from northern to southern regions, with the lowest and highest temperatures at Sta. SR22 in the northern Mendeleev Abyssal Plain and at Sta. M04 in the Chukchi Abyssal Plain, respectively.

The salinity of the three regions generally decreased from north to south. Salinity in the shallow continental shelf ranged from 29.43 to 31.99. Salinity at Stas SR03 and SR05 in the central waters was below 30.00. Salinity at Sta. SR01 in the southern Bering Strait, and at Stas SR08 and SR09 in the northern Herald shoal was above 31.0. Salinity in the continental slope was significantly lower than that in the shallow continental shelf, ranging from 26.96 to 27.68. The minimum and maximum salinity was recorded at Stas M07 and SR11, respectively. Salinity in the deep ocean ranged from 26.22 to 30.00. Salinity at Stas SR18, SR20 and SR22 in the northern Mendeleev Abyssal Plain exceeded 29.00. The salinity in remaining stations was below 28.00. The lowest salinity was observed at Sta. M05 in the south of Chukchi Abyssal Plain.

Nutrient concentrations in the three regions were higher in the return trip than in the departing trip. Nutrients in the shallow continental shelf were abundant, and higher in the southern Chukchi Sea compared with that in the northern Chukchi Sea. For example, the phosphate, DIN, and silicate values of Sta. SR01 were 0.94 μmol/L, 4.71 μmol/L, and 17.02 μmol/L, respectively, the highest observed in the shallow continental shelf, while nutrients at Stas SR08 and SR09 in the north of the Herald Shoal were the lowest for these respective nutrients in the shallow continental shelf. Nutrient content were relatively high in the continental slope and in the deep ocean, with small difference among stations. Phosphate concentration in these two regions was higher than that in the shallow continental shelf, while the concentrations of DIN and silicate were lower than that in the shallow continental shelf.

3.2 *Taxonomic composition and diversity of phytoplankton*

A total of 157 phytoplankton taxa (>5 μm) belonging to 69 genera were identified in the study area, including representatives of the following phyla of algae (Table A1): Cryptophyta (1), Katablepharidophyta (1), Haptophyta (1), Heterokontophyta (2), Bacillariophyta (99), Dinophyta (47), and Euglenophyta (6). Bacillariophyta was the dominant phytoplankton found in the western Arctic Ocean on this voyage, with numerous genera accounting for 62.13% of the total number of species and 95.86% of the total phytoplankton abundance. Dinophyta was the second most

abundant class of phytoplankton, accounting for only 29.94% of the total number of species and 3.26% of the total phytoplankton abundance. The abundances of other taxonomic groups were considerably lower, comprising only 0.88% of the total phytoplankton abundance. The dominant species were *Navicula pelagica* and *Thalassiosira nordenskioeldii*, accounting for 31.23% and 14.12% of the total phytoplankton abundance, respectively. The other frequently encountered species of diatoms with a station occurrence rate above 20% included *Chaetoceros diadema*, *Chaetoceros furcellatus*, *Leptocylindrus danicus*, *Thalassiosira rotula*, *Nitzschia longissima*, *Thalassionema nitzschioides*, *Navicula vanhoeffenii*, and *Cylindrotheca closterium*, accounted for more than 1% of the total phytoplankton abundance. The frequently encountered species of Dinophyta included *Gyrodinium fusiforme* and *Protoperidinium bipes*, with a station occurrence rate of 30% and 28%, respectively. However, the abundances only accounted for 0.2% and 0.1% of total phytoplankton abundance, respectively.

The species richness (d) of phytoplankton in the shallow continental shelf was the highest, while the lowest was recorded in the deep ocean, and decreased from low latitude to high latitude. In addition, the species richness (d) of phytoplankton during the departure trip was higher than that during the return trip (Table 1). A total of 137 phytoplankton species were found in the shallow-water zones at a depth of less than 500 m, while only 81 phytoplankton species were found in the deep-water zones at over a 500 m depth. The number of phytoplankton species at Stas R03 and CC01 in the southern Chukchi Sea reached more than 30. The number of species was especially high in the waters near the Herald Shoal in the northern Chukchi Sea. For example, Stas R09 in the northern Herald Shoal had the greatest number of 39. A total of 141 species of phytoplankton were found in the whole region during the departure trip, while only 84 species of phytoplankton were found in the whole region during the return trip.

3.3 *Horizontal distribution of phytoplankton abundance*

During the departure trip, the average phytoplankton abundance was as high as 797.07×10^2 cells/L. Along the shallow continental shelf, the average abundance was $(1\,467\pm3\,390)\times10^2$ cells/L (12.75×10^2–$13\,419.35\times10^2$ cells/L). Phytoplankton abundance was concentrated at Stas R08 and R09 at the edge of floating ice in the northern Herald Shoal. Station R09 had the maximum abundance ($13\,419.35\times10^2$ cells/L), which mainly consisted of *Navicula* spp. ($9\,053\times10^2$ cells/L), *Fragilariopsis* spp. ($2\,656\times10^2$ cells/L), *Thalassiosira* spp. (860×10^2 cells/L), and *Nitzschia* spp. (740×10^2 cells/L). These four genera accounted for 99.2% of the total abundance. The predominant species included *Navicula pelagica* ($7\,973\times10^2$ cells/L), *Fragilariopsis cylindrus* (940×10^2 cells/L), *Navicula vanhoeffenii* (813×10^2 cells/L), *Pesudo-nitzschia seriata* (287×10^2 cells/L), *Thalassiosira nordenskioeldii* (273×10^2 cells/L), and *Nitzschia longissima* (200×10^2 cells/L). The second highest abundance ($1\,827\times10^2$ cells/L) was located at Sta. CC01, which mainly included *Chaetoceros* spp. ($1\,545\times10^2$ cells/L) and *Leptocylindrus* spp. (75×10^2 cells/L), accounting for 84.6% and 4.1% of the station abundance, respectively. The coast of Alaska had poor nutrient and relatively low abundance. The values at Stas CC08, C02, and C06 were 128.5×10^2 cells/L, 105.5×10^2 cells/L, and 115.25×10^2 cells/L, respectively. In the northwest of Point Barrow, which had high ice coverage and low temperature, small areas of low abundance were observed. The abundance at Stas Co01, Co03, Co05, Co10, and C09 was all below 55×10^2 cells/L, with the lowest recorded at Sta. Co03 (12.75×10^2 cells/L). Phytoplankton abundance was dramatically lower in the continental slope, with a mean of $(51.88\pm5.48)\times10^2$ cells/L. The abundance at Stas Co05 and S23 were also relatively low, with 48.00×10^2 cells/L and 55.75×10^2 cells/L, respectively. The abundance in the deep ocean was even lower, with an average of $(27.65\pm18.67)\times10^2$ cells/L. The values at Stas S25, MS01, and MS02 were 6.75×10^2 cells/L, 13.0×10^2 cells/L, and 6.75×10^2 cells/L, respectively. Station Bn11, the northernmost station of the western Arctic Ocean, had more than 90% ice coverage, high salinity, and low temperature. The low temperature inhibits phytoplankton photosynthesis, leading to the abundance at only 7.50×10^2 cells/L. The seeding of ice algae to the water column at the center of the deep ocean resulted in abundances at Stas Bn05 and Bn06 of 50.0×10^2 cells/L and 66.5×10^2 cells/L, respectively, the latter representing the maximum abundance found in this region (Fig. 2).

During the return trip, the phytoplankton abundances declined significantly, with an average of 84.94×10^2 cells/L. Along the shallow continental shelf, the average abundance was $(223.1\pm275.7)\times10^2$ cells/L, ranging from 15.6 cells/L to 746.0×10^2 cells/L. Due to the early melting of sea ice in the southern Chukchi Sea, the upper layers of seawater had low nutrient content following high consumption of nutrients by phytoplankton. In addition, the enhancement of solar radiation maximized the surface temperature, which resulted in the formation of a strong halocline and blocked the transfer of nutrients to the surface layer from nutrient-rich deep waters, thereby reduced the abundance in the surface layer. Stations SR01, SR03, SR05, and SR07 had an abundance of less than 100×10^2 cells/L, with Sta. SR03 having the lowest value. While the abundance in the northern Chukchi Sea was more than 200×10^2 cells/L. Station SR08 had the highest abundance because its temperature and salinity were higher than that in the other stations. The phytoplankton bloom of eurythermal species *Cylindrotheca closterium* and *Protoperidinium bipes* caused the high abundance in Sta. SR08. The abundances of these species were 155×10^2 cells/L and 302.5×10^2 cells/L, accounting for 20.78% and 40.55% of the total abundance

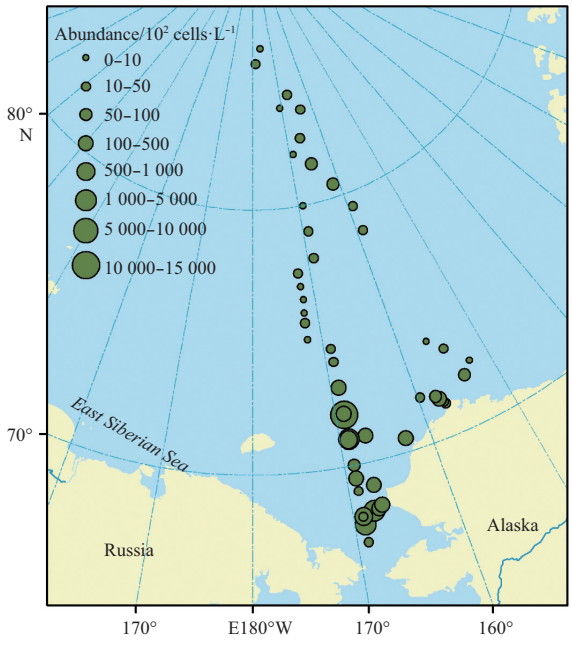

Fig. 2. Horizontal distribution of phytoplankton abundance in the surface waters.

at Sta. SR08, respectively. The average abundance in the continental slope was (12.41±6.29)×10^2 cells/L (range: 7.50×10^2–19.50×10^2 cells/L), which was significantly lower than that in the shallow continental shelf. The pattern of phytoplankton distribution was consistent with the patterns of temperature and salinity, with an increasing trend from northern to southern regions. The average abundance in the deep ocean was (9.70±7.99)×10^2 cells/L (range: 0.80×10^2–27.00×10^2 cells/L) and was lower than that in the shallow continental shelf and continental slope. As the sea ice coverage exceeded 70%, the northern Mendeleev Abyssal Plain had insufficient sunlight and low temperature, which affected the growth of autotrophic phytoplankton such as diatoms. Therefore, the abundance decreased below 10.0×10^2 cells/L at Stas SR22, SR20 and SR18, with Sta. SR22 having the lowest value. The Chukchi Abyssal Plain, located in the south of the deep ocean, had low sea-ice coverage (10%), resulted in the large amount of meltwater and low salinity of less than 27.0 at the seawater surface. Seawater stratification was more significant under these conditions, and blocked the replenishment of nutrients from the lower layers, thereby reduced the abundance in the upper layers. At the center of the deep ocean, ice coverage was approximately 30%. Ice algae released from melting sea ice had a seeding effect and significantly contributed to the relatively high phytoplankton abundance in this region (Fig. 2). In short, phytoplankton abundance decreased gradually from the shallow continental shelf to the continental slope and further in the deep ocean on both departure and return trips (Table 1).

3.4 *Vertical distribution of phytoplankton abundance in different regions*

The vertical distribution of phytoplankton abundance was noticeably different between each region. In the shallow continental shelf, Stas CC04 and SR10 were located in ice-free areas with depths of 51 m and 77 m, respectively. At Sta. CC04, the halocine and thermocline appeared at a depth of 20 m, with the water temperature decreasing from 5.83°C at a depth of 10 m to 3.39°C at 20 m, and salinity increased markedly from 31.86 at a depth of 10 m to 32.01 at 20 m. Nutrient concentration increased significantly at a depth of 30 m, where the phosphate value peaked. Phytoplankton abundance also peaked at a depth of 30 m at this station. At Sta. SR10, thermocline and halocline were found at a depth of 20 m. From depths of 10–20 m, the water temperature dropped dramatically from 2.32°C to –1.29°C, and the salinity increased observably from 30.09 to 31.90. Nutrient concentration gradually increased from the depth of 20 m to 75 m. The maximum phytoplankton abundance was found at a depth of 30 m at this station. Stations S23 and M07 were located in the continental slope with depths of 360 m and 381 m, respectively. Station S23 had more than 40% ice coverage, salinity increased gradually from the surface to the bottom, and there was no obvious thermocline or halocline. Phytoplankton abundance and nutrient concentration both peaked at a depth of 20 m at this station. At Sta. M07, where sampling was conducted during the return trip, the sea ice had completely melted away. Direct solar radiation and the melting of sea-ice caused the surface water to exhibit high temperatures and low salinity. The temperature gradually declined while salinity gradually increased in deeper layers; therefore, there was no thermocline or halocline at this station. Nutrient concentration increased significantly starting at the depth of 50 m and remained at a high level to the depth of 200 m. Phytoplankton abundance peaked at the depth of 50 m at this station. Stations Bn06 and M01 were located in the deep ocean with depths of 3 613 m and 2 310 m, respectively. Station Bn06 in the high-latitude had more than 90% ice coverage, while Sta. M01 in the mid-latitude had less than 30% ice coverage during the return trip. The findings at these two stations were similar, with temperature below 0°C at all depths, and no remarkable thermocline was found. Nutrients were abundant at all depths, increasing significantly from a depth of 50 m and remaining at a high level to a depth of 200 m; meanwhile, salinity increased dramatically at the depth of 50 m. Phytoplankton abundance also peaked at the depth of 50 m. In general, the maximum abundances were confined to the lower layers of the euphotic zone close to the layers of the halocline, thermocline, and nutricline. In the shallow continental shelf, the maximum abundance of phytoplankton occurred at depths below the halocline and thermocline. In the continental slope, the phytoplankton abundance peaked only in layers close to the nutricline. In the deep ocean, the phytoplankton abundance peaked in the deeper layers, which was consistent with the locations of the halocline and nutricline, but not correlated with water temperature (Fig. 3).

3.5 *Regional disparities of phytoplankton species succession*

The shallow continental shelf was located at lower latitude, and there was more than one month between the departure and return trips. Sea ice had completely melted by the return trip, the Pacific Ocean water of high temperature and salinity inflowed into this region unimpeded. In addition, direct solar radiation and adequate sunlight caused water temperature in the shallow continental shelf to increase significantly from (3.43±2.80)°C to (5.02±1.79)°C, so that there was wide spatial variability in the composition of the dominant phytoplankton species. Phytoplankton abundance decreased dramatically from (1 466.67±3 390)×10^2 cells/L to (223.12±275.68)×10^2 cells/L. Furthermore, the species composition changed markedly. During the departure trip, diatoms accounted for 96.74% of the total phytoplankton abundance, and pennate diatoms were the dominant group, pinnate diatoms and centric diatoms accounted for 64.98% and 35.02% of total diatom abundance, respectively. For example, the predominant species *N. pelagic* (443.90×10^2 cells/L) and *T. nordenskioedii* (201.23×10^2 cells/L), which belong to pennate and centric of diatoms, accounted for 31.28% and 14.18% of total diatom abundance, respectively. Dinoflagellates accounted for 1.88% of the total phytoplankton abundance. During the return trip, the proportion of diatoms increased to 98.04%, and centric diatoms were the dominant group, accounting for 70.6% of total diatom abundance. The predominant species *C. diadema* (130.80×10^2 cells/L) and *L. danicus* (26.50×10^2 cells/L) accounted for 59.79% and 12.11% of total diatom abundance, respectively. Whereas the proportion of pennate diatoms decreased to 29.4%. For example, the abundances of *N. pelagic* and *Cylindrotheca closterium* decreased to 16.21×10^2 cells/L and 10.40×10^2 cells/L, accounted for 7.41% and 4.75% of total diatom abundance, respectively. As the same time, the proportion of dinoflagellates in the total phytoplankton abundance decreased to 1.46%. In contrast, in the high latitude deep ocean, the time between the departure and return trips was short, and there was relatively small sea ice coverage change and all stations in the region were still covered with ice. The only significant change was that the thickness and extent of ice coverage declined between the two trips. Temperature at most stations in this region was below 0°C with a small decline between the trips, decreasing from (–1.19±0.55)°C to (–1.26±0.20)°C. There was small abundance variability in phytoplankton between the depart and return trips, decreasing from (27.65±18.67)×10^2 cells/L to (9.70±7.99)×10^2 cells/L, the range of variation was within the same level of magnitude. In addition, the

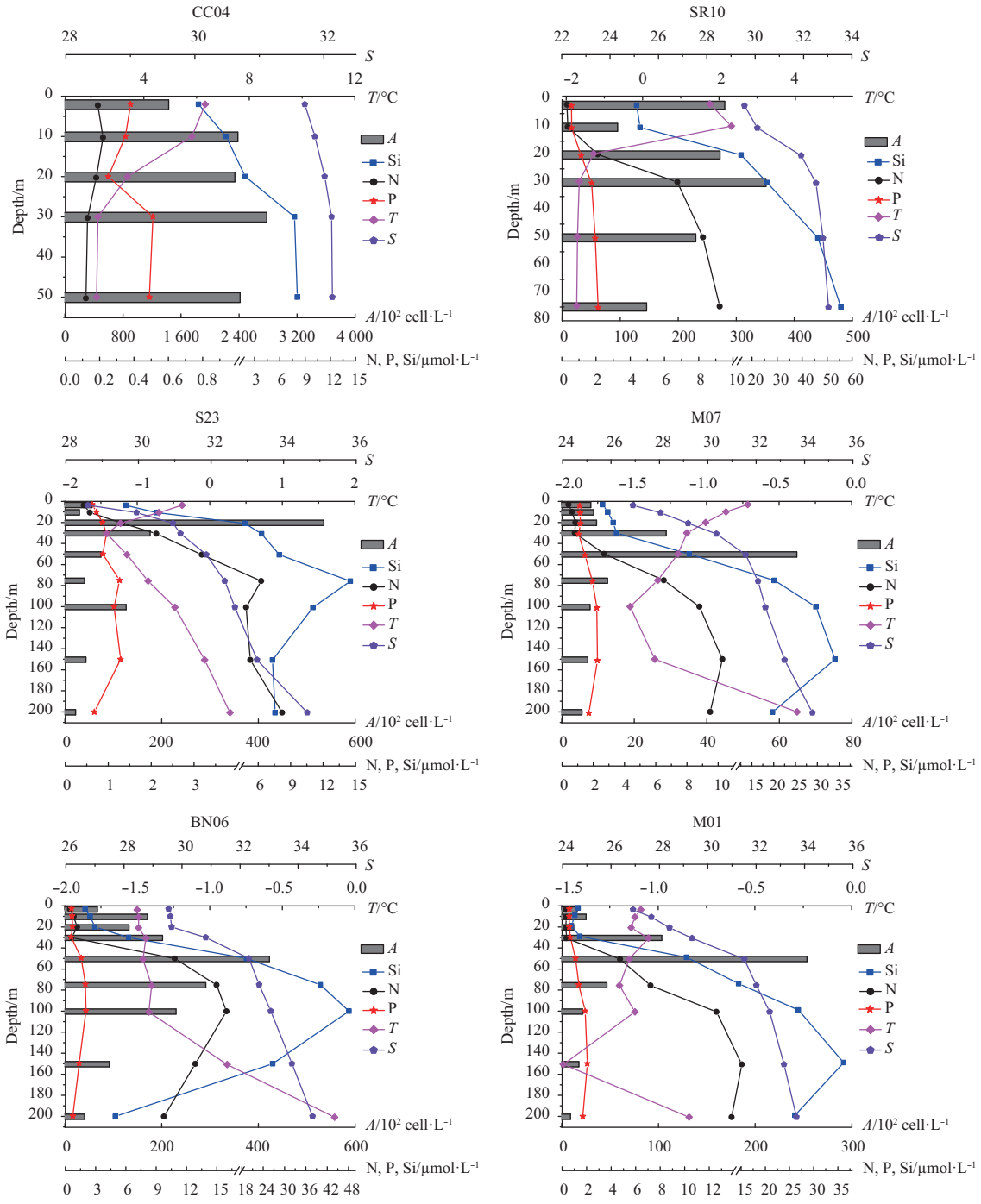

Fig. 3. Vertical distributions of temperature (*T*, °C), salinity (*S*), phosphate (P, μmol/L), DIN (N, μmol/L), silicate (Si, μmol/L), and phytoplankton abundance (*A*, 10^2 cells/L) in the western Arctic Ocean during the summer of 2010.

dominant genera of phytoplankton had small change between the two trips. The proportion of pennate diatoms decreased from 55.0% to 51.82% between the two trips, while that of centric diatoms increased from 33.2% to 35.6%, changes in the proportion of both genera occurred to a lesser extent in the deep ocean than in the shallow continental shelf. The dominant phytoplankton species was the same during the departure and return trips. *Thalassionema nitzschioides*, accounted for 12.4% and 7.71% of the total phytoplankton abundance, respectively. *Navicula* spp. accounted for 5.58% and 5.96%, and *Nitzschia* spp. accounted for 3.78% and 4.03% of the total abundance during the departure and return trips, respectively.

4 Discussion

4.1 *Relationship between phytoplankton distribution and environmental factors*

The average surface phytoplankton abundance of the entire sea area was 512.06×10^2 cells/L (range: 0.8×10^2 –13 419.35×10^2 cells/L). The highest abundance was observed in the north of the Herald Shoal, followed by the southern part of the Chukchi Sea. Phytoplankton abundance off the coast of Alaska on the east side

of the Chukchi Sea was significantly lower than on the west side of the Chukchi Sea. However, the abundance in the region northwest of Point Barrow was higher than off the coast of Alaska (Table 2). The spatial differences in the phytoplankton community in the western Arctic Ocean represent a characteristic feature of many aquatic environments. The southern Chukchi Sea connects to the Bering Sea via the Bering Strait. The western Chukchi Sea connects to the East Siberia Sea via the De Long Strait, and the eastern part connects to the Beaufort Sea in the northeast of Point Barrow. The northern part comprises the Chukchi Borderland as well as the Canadian Basin. The north central region of the Chukchi Sea is the Herald Shoal with a water depth of 30 m. The differences in the height between the Pacific Ocean and the Arctic Ocean drive the North Pacific Current. As a result, water with higher temperatures, salinity and nutrient content flows into the Chukchi Sea via the Bering Strait. The seawater inflow from the Pacific Ocean comprises three water masses. These include Anadyr Water from the west side of the strait (with low temperatures, high salinity, and high nutrient content), Alaska Coastal Water at the east side of the strait (with high temperatures, low salinity, and low nutrient content), and Bering Shelf Water in the middle of the strait (Coachman and Aagaard, 1988; Shi et al., 2004; Zhao et al., 2010). The seawater in the north of Herald Shoal is derived from Anadyr Water in the winter and early spring seasons, and exhibits low temperatures, high salinity, and high silicate content. In addition, the Herald Shoal has a significant effect on the motion of water mass and melting process of sea ice, and during sea ice melting, the seeding of ice algae and the enhancement of optical radiation stimulate ice-edge phytoplankton blooms (Heimdal, 1989; Zhao et al., 2010). Therefore, Sta. R09 in the north of Herald Shoal had lower temperature, lower salinity, and higher nutrient concentration than other stations of the shallow continental shelf. The temperature and salinity at Sta. R09 were as low as –1.224°C and 30.0, which were lower than the averages of the shallow continental shelf during the same period. Furthermore, the values of phosphate, DIN, and silicate were as high as 0.73 μmol/L, 0.53 μmol/L, and 11.67 μmol/L, respectively. In particular, the silicate concentration was significantly higher than the average of the shallow continental shelf during the same period (Table 1). In addition, ice algae released during ice melting had a seeding effect on phytoplankton blooms. For example, this region has higher populations of ice algae such as *Nitzschia frigida* than other areas. Therefore, the peak abundance of phytoplankton caused by ice-edge phytoplankton blooms was recorded at Sta. R09 in this study. Directly affected by the nutrient-rich Pacific water, the southern Chukchi Shelf represents an area of intensive development of phytoplankton throughout the spring and summer seasons (Grebmeier et al., 2006a; Sukhanova et al., 2009). The values of DIN and silicate in the shallow continental shelf were high during the departure trip despite high nutrient consumption by phytoplankton, similar to the values recorded during the return trip when ice was melting (Table 1). Stations CC01 and CC04 were located in the zone of a cyclonic circulation formed by the western branch of the Bering Sea Current in the southern Chukchi Sea. Owing to the regional features of the hydrophysical and hydrochemical regimes, Stas CC01 and CC04 in the southern Chukchi Sea had the second highest phytoplankton abundance. The narrow shelf of the Beaufort Sea receives considerable coastal runoff due to the Beaufort Gyre, which lowers the salinity of the nearshore waters and supplies a large amount of terrigenous material. Another possible reason for the formation of the high levels of phytoplankton abundance and biomass in the north-northwest of Point Barrow may lie in the upwelling that periodically occurs in this region and delivers deep water from the adjacent basin upward over the Barrow Canyon (Aagaard and Roach, 1990; Woodgate et al., 2005). In the present study, Sta. Co07 was located on the shelf of the Beaufort Sea in the northwestern Point Barrow. Affected by river freshwater input, it had a salinity of 0.61 lower than the average at the other stations on the east side of the Chukchi Sea (30.49). With the effect of upwelling, the temperature of Sta. Co07 was 3.52°C lower than the average at the other stations on the east side of the Chukchi Sea (2.22°C). In addition, there were abundant nutrients in both the upwelling and offshore currents. The overlaying and joining of these currents enhanced the phytoplankton abundance of Sta. Co07, which was an order of magnitude higher than other stations on the east side of the Chukchi Sea (Table 2). However, the phytoplankton abundance at Stas Co01, Co03, and Co05 was significantly lower than those from the west side of the Chukchi Sea due to its proximity to the coast of Alaska.

The relationship between environmental factors and phytoplankton was analyzed by CCA (Table 3). The first two axes explained 31.4% of the total variance in the phytoplankton abundance. Four significant canonical axes explained 33.4% of the phytoplankton variation. All canonical axes accounted for 58.7% of the variation in the phytoplankton data. We obtained a two-dimensional distribution figure of species, sample distribution, and environmental factors. The result showed that there were two distinct communities of phytoplankton in the Western Arctic Ocean: continental shelf community, which were positively correlated with temperature, encompassed samples collected in the Chukchi Shelf and the Alaska's northwest coast as well as Stas SR11and SR12 in the continental slope. The community was characteristic of high species diversity and abundance, and primarily dominated by neritic planktonic diatoms such as

Table 2. Correlations between phytoplankton distribution and environmental factors in the Chukchi Sea

	Regions								
	West side of the Chukchi Sea					East side of the Chukchi Sea			
	Southern Chukchi Sea			Northern Chukchi Sea		Coast of Alaska		Northwest of Point Barrow	
Station	R03	CC01	CC04	R08	R09	Co01	Co03	Co05	Co07
North latitude/(°)	68.00	67.67	68.13	71.01	71.96	71.25	71.33	71.42	71.50
West longitude/(°)	169.00	168.96	167.87	168.97	168.94	157.16	157.31	157.49	157.68
Salinity	31.87	32.00	31.70	30.36	30.00	30.46	31.00	30.02	29.88
Temperature/°C	4.99	5.06	6.33	0.85	–1.22	2.72	2.40	1.53	–1.30
Phosphate/μmol·L^{-1}	0.47	0.42	0.30	0.58	0.73	0.33	0.26	0.53	0.53
DIN/μmol·L^{-1}	0.33	0.27	0.20	0.23	0.53	0.62	0.83	0.67	0.97
Silicate/μmol·L^{-1}	0.04	0.01	0.95	19.00	11.67	0.70	0.87	0.27	1.28
Total abundance/10^2 cells·L^{-1}	916.50	1 827.02	1 430.00	4 503.50	13 419.35	26.50	12.75	48.00	338.00

Table 3. Canonical correspondence analysis results of phytoplankton

	Axes			
	1	2	3	4
Eigenvalues	0.308	0.236	0.022	0.014
Species–environment correlations	0.829	0.738	0.392	0.292
Cumulative percentage variance of species data	17.8	31.4	32.6	33.4
Cumulative percentage variance of species–environ relation	52.5	92.6	96.3	98.7
Sum of all eigenvalues	1.734			
Sum of all canonical eigenvalues	0.587			

Chaetoceros debilis, *C. diadema*, *Leptocylindrus danicus*, and *Nitzschia longissima*. Deep ocean community mainly distributed in abysmal sea and deep basin and affected directly by ice coverage. The assemblages of phytoplankton were represented by pennate diatoms such as *Navicula pelagic*, *Cylindrotheca closterium*, and *Thalassionema nitzschioides*. The latter community was subdivided into two groups; the first situated in Chukchi Abyssal Plain and Chukchi Cap as well as Stas Co05, S23 and M07 in continental slope; and the second situated in the Beaufort Sea, Mendeleev Abyssal Plain, and Alpha Ridge. Ice conditions worsened from the low latitude shelf to the high latitude basin as the voyage proceeded north, with the increase of ice coverage, the water temperature gradually decreased, and the two were negatively correlated. Thus, temperature and ice coverage were the most important environmental factors influencing phytoplankton distribution in the surveyed sea. Among the three types of nutrients, silicate had the largest effect on phytoplankton, which had significant influence on *Thalassiosira antarctica* and *T. nordenskioeldii* (Fig. 4). The above findings support the conclusion that light and water temperature are more important than nutriment for arctic phytoplankton (Heimdal, 1989; Lin et al., 2009). This clarifies the correlation between ecological characterization of phytoplankton and the environment. The entire western Arctic Ocean was not nutrient limited in this survey, DIN and phosphate was particularly abundant. For example, the concentrations of DIN and phosphate at Stas R09, where phytoplankton bloom occured, were as high as 0.53 μmol/L and 0.73 μmol/L, respectively (Table 2). Therefore, the effects of these two nutrients on phytoplankton were relatively small among the five environmental factors studied.

4.2 *Impact of melting ice on phytoplankton species composition*

Previous studies have reported the relationship between seasonal and inter-annual variations of Arctic phytoplankton species with sea ice conditions. With regard to the inter-annual variation, diatoms were dominated by a "sub-ice species", *Melosira arctica*, during a period of high ice cover in 1994 in the deep basins; however, during a period of low ice cover in 2008, it was dominated by "pelagic species" such as *Nitzschia* spp., *Fragilariopsis* spp., *Navicula* spp., and *Actinocyclus* spp. (Coupel et al., 2012). Regarding the seasonal variation, the phytoplankton species composition varied from spring to summer in the southern part of the Chukchi Sea. In early spring (May), the dominant species was the pennate diatom *Fragilaria striatula*. Two months later during summer, 97.5% of the phytoplankton were represented by the late-spring centric diatom *T. nordenskioeldii* (Sukhanova et al., 2009). Springer and McRoy (1993) also documented the dominance of the late-springtime and summertime diatom assemblages (*Chaetoceros* spp., *Thalassiosira* spp., and *Leptocylindrus* spp.) in this phytoplankton-rich region during summer. The species succession of Arctic phytoplankton was closely related to the sea ice conditions. Pennate diatoms such as *Navicula* spp. and *Fragilariopsis* spp. represent an important part of the algal community in Arctic ice. However, centric diatoms such as *Chaetoceros* spp., *Cylindrotheca* spp., and *Rhizosolenia* spp. are marine planktonic diatoms (Hsiao, 1980; Okolodkov, 1992; Booth and Horner, 1997). In the fjords of Svalbard, the relationship between ice type and the dominant algae species in the water column underneath shows that flagellates prevail under poor light conditions (thick ice, early in the season), while the dominant diatom *T. nordenskioeldii* appears later in the season at the ice-edge and in the open waters. The phytoplankton succession

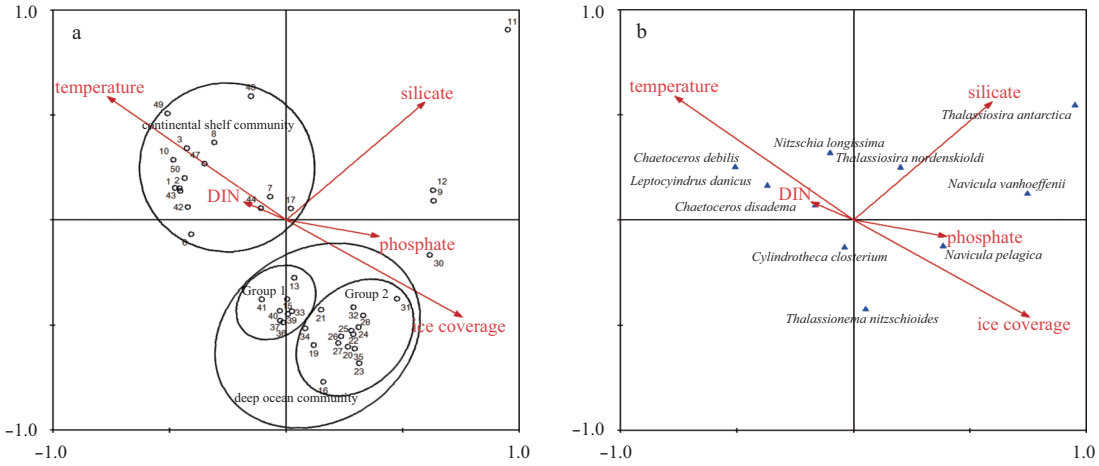

Fig. 4. Bi-plot of the canonical correspondence analysis (CCA) for sampling sites (circle) (a), diatom species (triangle) (b) and environmental factors (arrows) in the western Arctic Ocean.

could be summarized as a change from mostly heterotrophic flagellates to diatoms, followed later in the season by Dinophyceaes (Wiktor1999).

The present study reveals that even during the same season and at the same station, the phytoplankton species composition shows a significant rapid succession due to variations in sea ice conditions. Slightly more than a month elapsed between repeated sampling at the same stations during the return and departure trips. During the departure trip, Stas R08 and R09 were located at the ice-edge with sea ice of 1 m thick. Pennatae dominated the phytoplankton taxa, accounting for 73.05% and 83.35% of the total phytoplankton, respectively. *Navicula* spp. and *Fragilariopsis* spp. were the dominant species, accounting for 48.28% and 78.26% of the total phytoplankton abundance, respectively. However, during the return trip, Stas SR08 and SR09 were located in an ice-free region, with a drastic increase in water temperature. Centric diatoms became the dominant group of successional phytoplankton, accounting for 66.80% and 58.27%, respectively. *Chaetoceros* spp. and *Leptocylindrus* spp. were the dominant genera, accounting for 60.64% and 53.8% of the total abundance, respectively (Table 4). Due to global warming, the Arctic sea ice is quickly thinning and shrinking. The global consequences of greenhouse warming at polar latitudes are likely to show first in shallow adjacent seas of the Arctic Ocean, especifically the Pacific-influenced regions of the Chukchi Sea and East Siberian Sea (Walsh, 1989). Therefore, the Chukchi Sea is the region that is likely to most significantly manifest global climate change. This region is also ideal for studying the mechanisms of rapid changes in Arctic sea ice and the effects of climate change on marine ecosystems. The Arctic phytoplankton blooms are directly related to timing, duration, and location of ice melt. Sea ice coverage during the departure trip was higher than that during the return trip. Therefore, a comparison was made of the phytoplankton succession at the same locations to compare between the two trips, which reflected the response of phytoplankton to sea ice conditions. This study approach will be useful in determining both past and future changes in relation to predicted sea ice decline.

Table 4. Relationship between dominant phytoplankton species succession and ice conditions in repeated sample stations

		Station			
		R08	R09	SR08	SR09
	Investigation time	July 22, 2010	July 24, 2010	August 29, 2010	August 29, 2010
	Ice conditions	ice edge	ice edge	ice-free	ice-free
	Ice thickness/m	1	1	0	0
	Salinity	30.36	30.01	31.45	31.46
	Temperature/°C	0.85	–1.22	5.60	5.59
Pennatae	*Navicula* spp./%	28.94	58.46	0	0
	Fragilariopsis spp./%	19.34	19.80	0	0
	Nitzschia spp./%	13.44	2.96	4.68	21.44
	Pseudo-nitzschia spp./%	11.22	2.14	3.02	0
	Cylindrotheca spp./%	0	0	18.78	10.72
	other pennate diatoms/%	0.11	0	0	0.99
	total pennate diatoms/%	73.05	83.35	26.48	33.15
Centricae	*Chaetoceros* spp./%	5.66	1.12	49.25	15.28
	Leptocylindrus spp./%	0	0	11.39	38.52
	Thalassiosira spp./%	12.09	5.80	5.09	0
	other centric diatoms/%	0.51	0.38	1.07	4.46
	total centric diatoms/%	18.26	7.30	66.8	58.27

Acknowledgements

The authors thank Xiang Peng, Wang Yanguo and the arctic scientific investigation team aboard the icebreaker R/V *Xuelong* for collecting samples.

References

Aagaard K, Roach A T. 1990. Arctic Ocean-shelf exchange: measurements in Barrow canyon. Journal of Geophysical Research, 95(C10): 18163–18175

ACIA. 2005. Arctic Climate Impact Assessment. Cambridge: Cambridge University Press

Arrigo K R, van Dijken G, Pabi S. 2008. Impact of a shrinking Arctic ice cover on marine primary production. Geophysical Research Letters, 35(19): L19603

Bérard-Therriault L, Poulin M, Bossé L. 1999. Guide d'identification du phytoplancton marin de l'estuaire et du golfe du Saint-Laurent incluant également certains protozoaires. In: Canadian Special Publication of Fisheries and Aquatic Sciences No. 128. Ottawa: NRC Research Press

Booth B C, Horner R A. 1997. Microalgae on the Arctic Ocean section, 1994: species abundance and biomass. Deep Sea Research Part II: Topical Studies in Oceanography, 44(8): 1607–1622

Bursa A. 1963. Phytoplankton in coastal waters of the Arctic Ocean at Point Barrow, Alaska. Arctic, 16(4): 239–262

Coachman L K, Aagaard K. 1988. Transports through Bering Strait: annual and interannual variability. Journal of Geophysical Research, 93(C12): 15535–15539

Comiso J C, Parkinson C L, Gersten R, et al. 2008. Accelerated decline in the Arctic sea ice cover. Geophysical Research Letters, 35(1): L01703

Coupel P, Jin H Y, Ruiz-Pino D, et al. 2011. Phytoplankton distribution in the Western Arctic Ocean during a summer of exceptional ice retreat. Biogeosciences, 8(4): 6919–6970

Coupel P, Jin H Y, Joo M, et al. 2012. Phytoplankton distribution in unusually low sea ice cover over the Pacific Arctic. Biogeosciences, 9(2): 2055–2093

Cronin T M, Cronin M A. 2015. Biological response to climate change in the Arctic Ocean: the view from the past. Arktos, 1: 4

Fragoso G M, Poulton A J, Yashayaev I M, et al. 2016. Biogeographical patterns and environmental controls of phytoplankton communities from contrasting hydrographical zones of the Labrador Sea. Progress in Oceanography, 141: 212–226

Gosselin M, Levasseur M, Wheeler P A, et al. 1997. New measure-

ments of phytoplankton and ice algal production in the Arctic Ocean. Deep Sea Research Part II: Topical Studies in Oceanography, 44(8): 1623–1625
Grasshoff K, Kremling K, Ehrhardt M. 1999. Methods of Seawater Analysis. 3th ed. Chichester: John Wiley & Sons
Grebmeier J M. 2003. The western arctic shelf-basin interactions project. Arctic Research of the United States, 17: 24–36
Grebmeier J M, Cooper L W, Feder H M, et al. 2006a. Ecosystem dynamics of the Pacific influenced northern Bering and Chukchi Seas in the Amerasian arctic. Progress in Oceanography, 71(2-4): 331–361
Grebmeier J M, Harvey H R. 2005. The Western Arctic Shelf-Basin interactions (SBI) project: an overview. Deep Sea Research Part II: Topical Studies in Oceanography, 52(24-26): 3109–3115
Grebmeier J M, Overland J E, Moore S E, et al. 2006b. A major ecosystem shift in the northern Bering Sea. Science, 311(5766): 1461–1464
Hameedi M J. 1978. Aspects of water column primary productivity in the Chukchi Sea during summer. Marine Biology, 48(1): 37–46
Heimdal B R. 1989. Arctic Ocean Phytoplankton. In: Herman Y, ed. The Arctic Seas. New York: Van Nostrand Reinhold, 193–222
Hill V, Cota G. 2005. Spatial patterns of primary production on the shelf, slope and basin of the Western Arctic in 2002. Deep Sea Research Part II: Topical Studies in Oceanography, 52(24–26): 3344–3354
Hill V, Cota G, Stockwell D. 2005. Spring and summer phytoplankton communities in the Chukchi and Eastern Beaufort Seas. Deep Sea Research Part II: Topical Studies in Oceanography, 52(24-26): 3369–3385
Holland M M, Bitz C M, Hunke E C, et al. 2006a. Influence of the sea ice thickness distribution on polar climate in CCSM3. Journal of Climate, 19(11): 2398–2414
Holland M M, Bitz C M, Tremblay B. 2006b. Future abrupt reductions in the summer Arctic sea ice. Geophysical Research Letters, 33(23): L23503
Horner R. 1984. Phytoplankton abundance, chlorophyll a, and primary production in the western Beaufort Sea. In: Barnes P W, Shell D M, Reimnitz E, eds. The Alaskan Beaufort Sea: Ecosystems and Environments. New York: Academic Press, 295–310
Hsiao S I C. 1980. Quantitative composition, distribution, community structure and standing stock of sea ice microalgae in the Canadian Arctic. Arctic, 33(4): 768–793
Hunt Jr G L, Stabeno P, Walters G, et al. 2002. Climate change and control of the southeastern Bering Sea pelagic ecosystem. Deep Sea Research Part II: Topical Studies in Oceanography, 49(26): 5821–5853
Joo H M, Lee S H, Jung S W, et al. 2012. Latitudinal variation of phytoplankton communities in the Western Arctic Ocean. Deep Sea Research Part II: Topical Studies in Oceanography, 81-84: 3–17
Kiselev I A. 1937. Composition and distribution of phytoplankton in the northern part of the Bering Sea and southern part of the Chukchi Sea. In: Investigations of the Seas of the USSR (in Russian). Leningrad, Moscow: Hydrometeoizdat Publishing, 217–245
Kwok R, Rothrock D A. 2009. Decline in Arctic sea ice thickness from submarine and ices at records: 1958-2008. Geophysical Research Letters, 36(15): L15501
Le Fengfeng, Hao Qiang, Jin Haiyan, et al. 2014. Size structure of standing stock and primary production of phytoplankton in the Chuchi Sea and the adjacent sea area during the summer of 2012. Haiyang Xuebao (in Chinese), 36(10): 103–115
Lee R E. 2008. Phycology. 4th ed. Cambridge: Cambridge University Press
Li W K W, McLaughlin F A, Lovejoy C, et al. 2009. Smallest algae thrive as the Arctic Ocean freshens. Science, 326(5952): 539
Lin Gengming, Yang Qingliang, Tang Senmning. 2009. Relationship between phytoplankton distribution and environmental factors in the Chukchi Sea. Marine Science Bulletin, 11(2): 55–63
Lin Gengming, Wang Yu, Yang Qingliang. 2013. Species diversity of phytoplankton communities in the Western Arctic Ocean during summer 2010. Biodiversity Science (in Chinese), 21(5): 527–536
Liu Zilin, Chen Jianfang, Zhang Tao, et al. 2007. The size-fractionated chlorophyll *a* concentration and primary productivity in the Chukchi Sea and its northern Chukchi Plateau. Acta Ecologica Sinia, 27(12): 4953–4962
Liu Zilin, Chen Jianfang, Liu Yanlan, et al. 2011. The size-fractionated chlorophyll *a* and primary productivity in the surveyed area of the western Arctic Ocean during the summer of 2008. Haiyang Xuebao (in Chinese), 33(2): 124–133
Okolodkov Ju V. 1987. Planktonic algae of the Chukchi Sea [dissertation] (in Russian). Leningrad: Komarov Botanical Institute, Russian Academy of Sciences
Okolodkov Y B. 1992. Cryopelagic flora of the Chukchi, East Siberian and Laptev Seas. Proceedings of the NIPR Symposium on Polar Biology, 5: 28–43
Overland J E, Wang M Y. 2007. Future regional Arctic sea ice declines. Geophysical Research Letters, 34(17): L17705
Pabi S, van Dijken G L, Arrigo K R. 2008. Primary production in the Arctic Ocean, 1998-2006. Journal of Geophysical Research, 113(C8): C08005
Perovich D K. 2011. The changing Arctic sea ice cover. Oceanography, 24(3): 162–173
Polyakov I V, Timokhov L A, Alexeev V A, et al. 2010. Arctic Ocean warming contributes to reduced polar ice cap. Journal of Physical Oceanography, 40(12): 2743–2756
Round F E, Crawford R M, Mann D G. 1990. The Diatoms: Biology and Morphology of the Genera. Cambridge, UK: Cambridge University Press, 1–747
Sergeeva V M, Sukhanova I N, Flint M V, et al. 2010. Phytoplankton community in the Western Arctic in July-August 2003. Oceanology, 50(2): 184–197
Shi Jiuxin, Zhao Jinping, Jiao Yutian, et al. 2004. Pacific inflow and its links with abnormal variations in the Arctic Ocean. Chinese Journal of Polar Research (in Chinese), 16(3): 253–260
Springer A M, McRoy C P. 1993. The paradox of pelagic food webs in the northern Bering Sea: III. Patterns of primary production. Continental Shelf Research, 13(5-6): 575–599
Stroeve J C, Serreze M C, Fetterer F, et al. 2005. Tracking the Arctic's shrinking ice cover: another extreme September minimum in 2004. Geophysical Research Letters, 32(4): L04501
Sukhanova I N, Flint M V, Pautova L A, et al. 2009. Phytoplankton of the western arctic in the spring and summer of 2002: structure and seasonal changes. Deep Sea Research Part II: Topical Studies in Oceanography, 56(17): 1223–1236
Sun Jun, Liu Dongyan. 2002. The preliminary notion on nomenclature of common phytoplankton in China seas waters. Oceanologia et Limnologia Sinica (in Chinese), 33(3): 271–286
Tomas C R. 1997. Identifying Marine Phytoplankton. San Diego: Academic Press, 1–858
Utermöhl H. 1958. Zur vervollkommung der quantitativen phytoplankton-methodik. Mitteilungen der Internationale Vereinigung für Theoretische und Angewandte Limnologie, 9: 1–38
Walsh J J. 1989. Arctic carbon sinks: present and future. Global Biogeochemical Cycle, 3(4): 393–411
Wang J, Cota G F, Comiso J C. 2005. Phytoplankton in the Beaufort and Chukchi Seas: distribution, dynamics, and environmental forcing. Deep Sea Research Part II: Topical Studies in Oceanography, 52(24-26): 3355–3368
Wassmann P, Duarte C M, Agustí, S, et al. 2011. Footprints of climate change in the Arctic marine ecosystem. Global Change Biology, 17(2): 1235–1249
Wiktor J. 1999. Early spring microplankton development under fast ice covered fjords of Svalbard, Arctic. Oceanologia, 41(1): 51–72
William K W, McLaughlin F A, Lovejoy C, et al. 2009. Smallest algae thrive as the Arctic Ocean freshens. Science, 326: 539, doi: 10.1126/science.1179798
Woodgate R A, Aagaard K, Weingartner T J. 2005. A year in the physical oceanography of the Chukchi Sea: moored measurements from autumn 1990-1991. Deep Sea Research Part II: Topical

Studies in Oceanography, 52(24-26): 3116–3149

Yang Qingliang, Lin Gengming, Lin Mao, et al. 2002. Species composition and distribution of phytoplankton in Chukchi Sea and Bering Sea. Chinese Journal of Polar Research (in Chinese), 14(2): 113–125

Yang Qingliang, Lin Gengming. 2006. A multivariate analysis of net-phytoplankton assemblages in the Chukchi Sea and Bering Sea. Chinese Journal of Plant Ecology (in Chinese), 30(5): 763–770

Zapata M, Rodríguez F, Garrido J L. 2000. Separation of chlorophylls and carotenoids from marine phytoplankton: a new HPLC method using a reversed phase C_8 column and pyridine-containing mobile phases. Marine Ecology Progress Series, 195: 29–45

Zhang Fang, He Jianfang, Lin Ling, et al. 2015. Dominance of picophytoplankton in the newly open surface water of the central Arctic Ocean. Polar Biology, 38(7): 1081–1089

Zhao Jinping, Shi Jiuxin, Jin Mingming, et al. 2010. Water mass structure of the Chukchi Sea during ice melting period in the summer of 1999. Advances in Earth Science (in Chinese), 25(2): 154–162

Appendix:

Table A1. Predominant species of the phytoplankton found in the Western Arctic Ocean during the summer of 2010

	Species
I Bacillariophyta	*Chaetoceros brevis* Schütt, 1895
	Chaetoceros concavicornis Mangin, 1917
	Chaetoceros decipiens Cleve, 1873
	Chaetoceros diadema (Ehrenberg) Gran, 1897
	Chaetoceros furcellatus Bailey, 1856
	Chaetoceros laciniosus F. Schütt, 1895
	Cylindrotheca closterium (Ehrenberg) Reimann et Lewin, 1839
	Fragilariopsis cylindrus (Grunow) Krieger, 1954
	Fragilariopsis oceanica (Cleve) Hasle, 1965
	Leptocylindrus danicus Cleve, 1889
	Leptocylindrus minimus Gran, 1915
	Navicula pelagica Cleve, 1896
	Navicula vanhoeffenii Gran, 1897
	Nitzschia frigida Grunow, 1880
	Nitzschia longissima (Brébisson) Ralfs, 1861
	Pseudo-nitzschia seriata (Cleve) H. Peragallo, 1900
	Proboscia alata (Brightwell) Sundström, 1986
	Rhizosolenia hebetata f. *semispina* (Hansen) Gran, 1908
	Rhizosolenia setigera Brightwell, 1858
	Thalassiosira antarctica Comber, 1896
	Thalassiosira nordenskioeldii Cleve, 1873
	Thalassiosira rotula Meunier, 1910
	Thalassionema nitzschioides (Grunow) Mereschkowsky, 1902
II Dinophyta	*Alexandrium ostenfeldii* (Paulsen) Balech et Tangen, 1904
	Alexandrium tamarense (Lebour) Balech, 1995
	Amphidinium extensum Wulff, 1916
	Amphidinium sphenoides WüIff, 1916
	Dinophysis norvegica Claparède & Lachmann, 1859
	Gyrodinium fusiforme Kofoid & Swezy, 1921
	Gyrodinium wulffii Schiller, 1933
	Gyrodinium pingue (Schütt) Kofoid & Swezy, 1921
	Gymnodinium arcticum Wulff, 1919
	Gymnodinium simplex (Lohmann) Kofoid & Swezy, 1921
	Protoperidinium bipes (Paulsen) Balech, 1974
	Protoperidinium brevipes (Paulsen) Balech, 1974
	Protoperidinium pellucidum Bergh, 1881
	Scrippsiella trochoidea (Stein) Loeblich III, 1976
III Euglenophyta	*Eutreptia lanowii* Steuer, 1904
	Eutreptiella braarudii Throndsen, 1969
	Eutreptiella gymnastica Throndsen, 1969